Enhancement of X-Ray Power from a *Z* Pinch Using Nested-Wire Arrays

C. Deeney, M. R. Douglas, R. B. Spielman, T. J. Nash, D. L. Peterson,* P. L'Eplattenier,† G. A. Chandler, J. F. Seamen, and K. W. Struve

Sandia National Laboratories, MS-1194, P.O. Box 5800, Albuquerque, New Mexico 87185

(Received 28 May 1998)

Nested-wire arrays on the 20-MA *Z*-pinch accelerator have produced x-ray powers up to 280 ± 40 TW (a 40% increase over a single array) and an x-ray pulse width of 4 ns. The short x-ray pulse widths are associated with the formation of tight (1-mm-diameter), uniform pinches at stagnation. Two-dimensional radiation magnetohydrodynamic calculations suggest that the inner array mitigates the growth of implosion instabilities thereby leading to smaller diameter pinches that radiate at higher power than single-wire arrays. [S0031-9007(98)07768-0]

PACS numbers: 52.55.Ez, 52.25.Nr, 52.50.Lp, 52.65.Kj

Recently, *Z* pinches have demonstrated remarkable results in radiated energies and powers due to improved symmetry and mitigation of Rayleigh-Taylor instabilities [1–5]. On the 20 MA *Z* facility [5] at Sandia National Laboratories (SNL), tungsten wire array implosions have generated very high (200 TW) power [5] relevant for applications to inertial confinement fusion (ICF) [4,6], laboratory astrophysics measurements [7], radiation-material interactions [8], high-energy photon production, and the generation of unique plasma states.

We believe that one of the primary impediments to achieving higher x-ray power is the onset of acceleration-driven Rayleigh-Taylor instabilities and asymmetries during the implosion [1–5]. The most common technique that has been proposed to mitigate these instabilities is to introduce additional mass to the shell as it implodes [9–12]. This technique has been tried experimentally by Baskht *et al.* [13] using multiple gas puff shells. In this paper, we report for the first time the use of nested-wire arrays. Nested-wire arrays on the 20-MA *Z* accelerator at SNL have produced x-ray powers up to 280 ± 40 TW, have reduced the total x-ray pulse width from 5.8 to 4 ns, and have produced pinched plasmas with diameters of only 1 mm with good axial uniformity. We will present this data along with two-dimensional radiation magnetohydrodynamic (MHD) calculations.

It was not clear from the outset that the multiple shell configurations would lead to higher radiated powers for wire arrays. Theoretical work by Douglas *et al.* [14] and Davis *et al.* [15] had suggested that either in a plasma shell regime or in an individual wire regime, respectively, nested arrays could modify and possibly improve implosion quality. For imploding *Z* pinches the advantage of an internal array can be described by two mechanisms, depending on whether the outer wire array forms a complete shell as it implodes or remains as individual current carrying filaments. If the outer array becomes a shell as it implodes, then the growth of the RT instability leads to millimeter wavelength bubble and spike structures, which redistributes mass both radially and axially on this inwardly accelerating plasma. The stagnation of the shell on an unperturbed (i.e., noncurrent carrying) inner shell can slow the growth rate of the RT and, depending on the inner shell thickness and density, significantly reduce the amplitude of the instability. The bubble front decelerates which allows the spikes to "catch up," resulting in a narrower sheath. If, on the other hand, the wires remain discrete, then a current commutation may occur when the outer array passes through the inner array due to inductive effects [15,16]. Davis *et al.* have speculated that the higher rate of rise of current seen by the inner array, at the time of commutation, could produce a higher quality pinch.

A photograph of a nested-wire array is shown in Fig. 1. This nested array is composed of a 40-mm-diameter outer array with 240 wires, surrounding a 20-mm-diameter inner array of 120 wires. The two arrays, the anode and the cathode, are marked in Fig. 1: The three central rods are alignment devices. The array is inserted into the anode-cathode gap of the power feed structure on *Z*. The 36 modules of the *Z* accelerator deliver a 50-TW, 20-MA, 3-MJ electrical pulse into the vacuum region. Typically, 18 to 19 MA of current is delivered to the array in a 100 ns time-to-peak current. The radiation emissions are

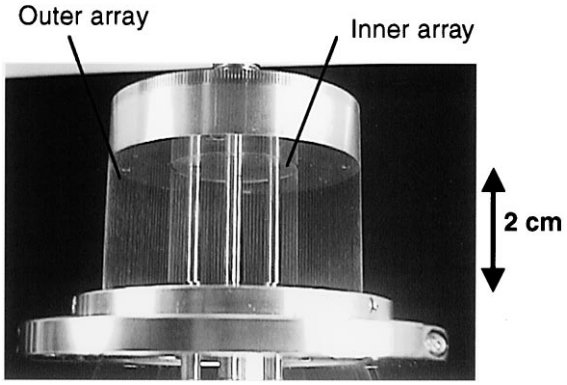

FIG. 1. A photograph of a 40-mm outer diameter, 20-mm inner diameter nested array.

measured with nickel bolometers, a calorimeter, a time-resolved pinhole camera with 100-ps, 100-μm resolution, and an array of filtered x-ray diodes. These detectors are discussed in Ref. [5] and the references therein.

In Table I, all nested wire data are summarized from three scans with the nested configuration on the Z accelerator. The first scan involved adjusting the mass on the outer and inner arrays to ensure a similar implosion time to a single-wire array; i.e., as the outer mass was decreased, the inner mass was increased. In principle, the same implosion times should translate to similar energy coupling to the pulsed power driver; unfortunately, there was evidence of reduced coupling with the lightest outer arrays. The second scan left the mass of the outer array constant as the mass of the inner array was increased from approximately 25% to 100% of that of the outer array. By keeping the outer array configuration constant, the level of instability growth would be the same, within shot-to-shot variations, at the time of impact onto the inner array. This would clarify the role of the mass of the inner shell. To investigate wire number effects, the third varied the wire number in the inner array while maintaining a nearly constant inner array mass. For comparison to these nested array results, the data from typical 40-mm-diameter arrays composed of 240, 7.5-μm-diameter wires are included in the table. This single-array configuration produced the highest powers, shortest pulse widths, and tightest compressions when compared to single arrays covering a wide range of masses, wire numbers, and diameters.

In Fig. 2 we illustrate the dynamics of the implosion of a nested-array shot, Z179 using a zero-dimensional (0D) implosion model coupled with a circuit code. Shot Z179 was the highest power shot with a measured peak power of 280 $\pm$ 40 TW in a 4 ns FWHM radiation pulse. The total radiated energy was 1.75 $\pm$ 0.20 MJ. At approximately 95 ns into the current pulse, the zero-dimensional calculation predicts that the outer array reaches the inner array as illustrated in Fig. 2, where a sharp drop in the calculated implosion velocity (dash-dotted curve) is seen due to the conservation of momentum. Both the calculated magnetically insulated transmission line (MITL) current (dashed curve) and load current (dotted curve) are also plotted in Fig. 2. The measured MITL current and x-ray powers are shown for comparison, both as solid curves, in Fig. 2. The measured x-ray power exhibits an increase (a step) at approximately the same time (95 ns) as the 0D implosion model would have predicted the strike of the outer array with the inner array. We are assuming, based on two-dimensional radiation-MHD calculations using the code described in Ref. [17], that the impact of the outer and inner shells will result in an increase in the x-ray emissions. The time for the ensemble to reach the minimum radius is 118 ns, as determined by the peak in the x-ray power and a minimum in the x-ray pinhole image. This is in agreement with the calculated implosion time.

Time-resolved x-ray pinhole photography indicates that the increased radiated power and decreased x-ray pulse width is associated with a marked improvement in the tightness and uniformity of the imploded plasma. In Fig. 3, the image of the pinch at peak power for a nested array is shown, along with an equivalent image for a single array, which produced 200 TW in a 5.8 ns FWHM pulse. It is apparent from the radial lineouts in Fig. 3 that the minimum diameter of 1.0 $\pm$ 0.1 mm achieved with a nested array is smaller than the tightest single array implosions of 1.5 $\pm$ 0.1 mm. In addition, the data in Table I indicate that the shorter x-ray pulses correlate with tighter implosions.

The improved pinch quality may be explained by 2D radiation-MHD code [18] calculations which invoke RT

TABLE I. A summary of the nested-wire arrays with a 40-mm outer diameter array and a 20-mm inner diameter array.

Shot	Outer mass (μg/cm)	Inner mass (μg/cm)	Inner wire number	Implosion time (ns)	X-ray FWHM (ns)	X-ray power (TW)	X-ray energy (kJ)	Pinch diam (mm)
Single array								
161	2054	0	0	112	5.8	195	1700	1.5 $\pm$ 0.2
Constant implosion time scan								
140	1846	471	120	109	4.8	250	1800	NA
163	1846	471	120	110	5.3	220	1650	1.6 $\pm$ 0.2
142	1472	1443	120	112	5.4	180	1500	1.2 $\pm$ 0.1
141	1359	1826	120	109	5	170	1400	1.5 $\pm$ 0.1
143	942	2633	120	110	8.5	100	1500	2.2 $\pm$ 0.2
Constant outer array mass scan								
178	1846	471	120	115	5.3	200	1500	1.3 $\pm$ 0.1
179	1846	1027	120	119	4	280	1750	1.0 $\pm$ 0.1
180	1846	1446	120	118	4.2	260	1500	1.0 $\pm$ 0.1
181	1846	1899	120	125	4	230	1650	1.0 $\pm$ 0.1
Inner array wire number scan								
182	1846	513	240	117	5.5	220	1700	1.7 $\pm$ 0.1
186	1846	584	60	118	5.7	210	1600	1.5 $\pm$ 0.1

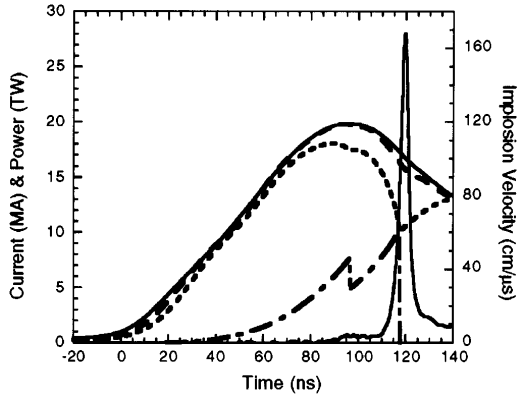

FIG. 2. An overlay of the measured (solid curves) MITL current and x-ray power pulse for Z179. The calculated MITL current (dashed curve), load current (dotted curve), and outer shell implosion velocity (dash-dotted curve) are also plotted.

mitigation [14]. The calculated evolution of a single shell and a double shell implosion are illustrated in Fig. 4 where isodensity contour plots are shown for three different times during the implosion. In this figure, the stagnation of the outer shell onto the inner shell is found to reduce the amplitude of the RT and hence shell thickness, by a factor of 2 when compared to a single array at the same time (105 ns). This decreases shell thickness will lead to tighter pinches and narrower x-ray pulse widths. The data in Table I show that the nested shell implosions clearly produce narrower FWHMs and tighter pinches than the single arrays. This is especially true for the constant outer mass scan.

The contrast between the optimized nested implosions and the best single array implosions is evident in Fig. 5, where the normalized x-ray powers for shot Z179 (solid curve) and for Z161, a single array (dash-dotted curve), are overlayed. Because of the additional mass of the inner array, the peak x-ray power for Z179 occurred some 7 ns after the peak in Z161. We have time shifted Z161 to match the peaks. The presence of the inner shell causes an increase (step) in the x-ray power during the run in phase due to the strike. The measured step is lower in amplitude and broader in time than that predicted by a 2D radiation-MHD [17] calculation which is shown as the

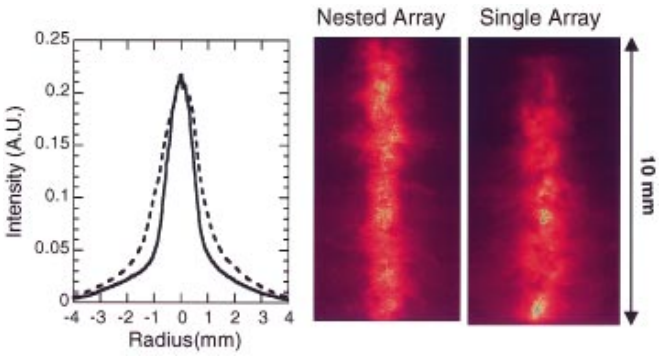

FIG. 3(color). Two 100-ps duration, 150-μm spatial resolution images, filtered with 4 μm of Kimfol, are shown for a nested and a single array. The z-axis-averaged, radial lineouts of the intensities for both are also plotted.

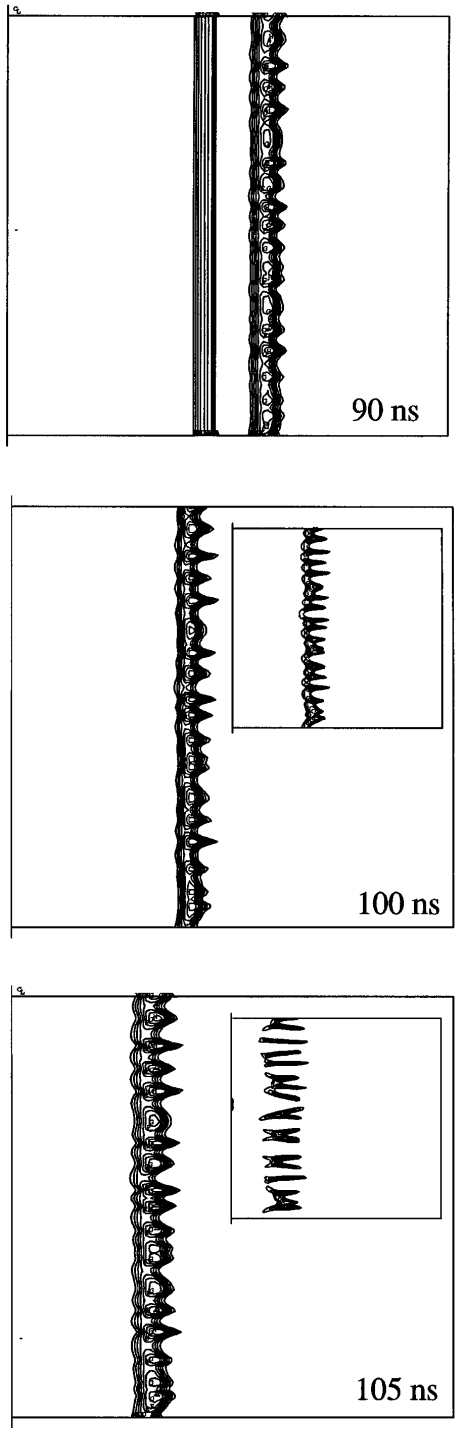

FIG. 4. Three isodensity contours' time from a MACH2 2D radiation-MHD calculation of a nested-wire array implosion (Z179). These density contours show that the inner layer reduces the amplitudes of the Rayleigh-Taylor instabilities prior to stagnation when compared to a single array, shown as insets.

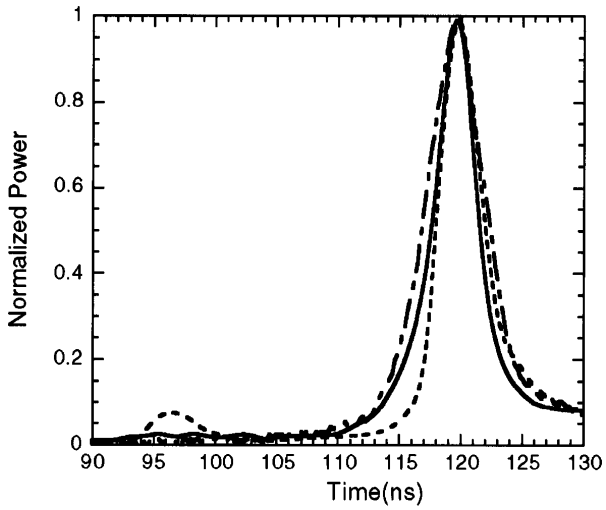

FIG. 5. An overlay of the normalized powers for Z179 (solid curve) with the normalized powers for Z161, a 40-mm-diameter single array (dot-dashed curve), and for a 2D radiation-MHD calculation (dotted curve).

dotted curve in Fig. 5. This discrepancy may be due to the thickness of the inner and/or outer shell being larger than the 1-mm thickness that was used in the calculation, or it could be due to the outer and inner arrays still being composed of discrete but expanded wires. In reference to this latter hypothesis, it should be noted, however, that the observed x-ray pulse widths listed in Table I did not change markedly for the shots where the number of wires in the inner wire array were varied from 60 to 120 to 240 for a near constant mass. Calculations are underway to study wire effects [16]. Based on the wire number scan data, however, the shell thickness hypothesis seems more likely.

The 2D calculations plotted in Fig. 5 reproduces the pulse width reductions. This match was obtained by using the same initial parameters as were employed to reproduce the single array implosions, and by the inclusion of a 1-mm thick, unperturbed inner shell located at a 20-mm diameter. The reduction in pinch size is also seen in the calculations; for example, a 1.6-mm diameter is calculated for a single array (Z51 or 161), and a 1.0 mm diameter is calculated for nested arrays such as Z179 and Z180. The 2D calculation does predict a higher power (340 TW) than the measured value, and it also predicts a faster rise time than the observed rise time. Again, these differences may be due to inadequate knowledge of the conditions of the inner and outer plasmas at their impact. Further modeling of these implosions, including mode structure analyses and current commutation effects, needs to be performed.

In summary, we report on a series of nested tungsten wire array implosions. The optimum performance as determined by the highest powers and shortest x-ray pulse widths were achieved with an inner array of wires, at 50% of the outer array's diameter, and with 50% of the outer array's mass. With this configuration, 40% power increases, 30% reductions in pulse width, and a factor of 1.5 reduction in final pinch diameter were measured. Such improvements have been explained by 2D radiation-MHD calculations that suggest the RT is mitigated by the inclusion of an inner shell. The resulting increases in x-ray powers and inferred improvements in implosion quality will be beneficial to many of the applications of *Z* pinches. Future experiments and calculations will study the optimization of the materials, number of wires, and location of the inner shell(s) plus investigate the details of the strike phase.

We acknowledge beneficial discussions with A. Velikovich, R. Terry, and J. Davis of NRL, N. Roderick of UNM, R. Benattar of Ecole Polytechnique, and J. Hammer of LLNL. We also thank the *Z* crew for their outstanding technical support.

*Permanent address: Los Alamos National Laboratory, Los Alamos, NM 87545.
†Permanent address: DT/HP-Centre d'Etude de Gramat, 46500 Gramat, France.

[1] C. Deeney *et al.,* Phys. Rev. E **56**, 5945 (1997).
[2] T. W. L. Sanford *et al.,* Phys. Rev. Lett. **77**, 5063 (1996).
[3] M. R. Douglas, C. Deeney, and N. Roderick, Phys. Rev. Lett. **78**, 4577 (1997).
[4] M. K. Matzen, Phys. Plasmas **4**, 1519 (1997).
[5] R. B. Spielman *et al.,* Phys. Plasmas **5**, 2105 (1998).
[6] V. P. Smirnov, Plasma Phys. Controlled Fusion **33**, 1697 (1991); J. Lindl, Phys. Plasmas **2**, 3933 (1995).
[7] P. T. Springer *et al.,* J. Quant. Spectrosc. Radiat. Transfer **58**, 927 (1997).
[8] R. E. Olson *et al.,* Phys. Plasmas **4**, 1818 (1997).
[9] S. M. Gol'berg and A. L. Velikovich, Phys. Fluids B **5**, 1164 (1993).
[10] A. L. Velikovich, F. L. Cochran, and J. Davis, Phys. Rev. Lett. **77**, 853 (1996).
[11] J. H. Hammer *et al.,* Phys. Plasmas **3**, 2063 (1996).
[12] D. L. Book, Phys. Plasmas **3**, 354 (1996).
[13] R. B. Baksht *et al.,* Plasma Phys. Rep. **21**, 907 (1995).
[14] M. R. Douglas *et al.,* Bull. Am. Phys. Soc. **42**, 1878 (1997).
[15] J. Davis, N. A. Gondarenko, and A. L. Velikovich, Appl. Phys. Lett. **70**, 170 (1997).
[16] Robert E. Terry (private communication).
[17] D. L. Peterson *et al.,* "Characterization of Energy Flow and Instability Development in 2-D Simulations of Hollow Z-Pinches," Phys. Plasmas (to be published).
[18] R. E. Peterkin, Jr., *et al.,* IEEE Trans. Plasma Sci. **21**, 552 (1993).